Cosmic ray positron and antiproton production in supernova remnants

E.G. BEREZHKO, L.T. KSENOFONTOV.

Yu.G. Shafer Institute of Cosmophysical Research and Aeronomy, 31 Lenin Ave., 677980 Yakutsk, Russia.

ksenofon@ikfia.ysn.ru

Abstract: We study the production of cosmic rays (CRs) in supernova remnants (SNRs), including the production of electron, positron and antiproton CR components. This combines nuclear collisions inside CR sources and in the diffuse interstellar medium leading to the creation of electrons, positrons and antiprotons, as well as their reacceleration, with the injection and subsequent acceleration of suprathermal protons and electrons from the postshock thermal pool. Selfconsistent CR spectra are calculated on the basis of the nonlinear kinetic model. Results of calculations will be presented. Calculated spectra are in the satisfactory agreement with the existing measurements.

Keywords: acceleration of particles, cosmic rays, shock waves

1 Introduction

The Galactic cosmic rays (CRs), with proton energies below a few 10^{15} eV, are generally believed to be accelerated in supernova remnants (SNRs)(e.g. [1]). Nonlinear kinetic theory of CR acceleration in SNRs [2, 3, 4] is consistent with observational data available at the time. This includes the energy spectra of CR nuclei and the properties of nonthermal emission produced by CRs inside SNRs. Therefore one can use the term "standard model" for this theory.

Considerations based on the selfconsistent kinetic nonlinear model for CR acceleration in SNRs show that the reacceleration of the existing Galactic CRs (GCRs) and the creation of secondary CRs species due to the collisions of primary CRs with the gas nuclei in SNRs strongly influence the energy spectra of secondary elements, like Li, Be, B [5]. Due to this additional mechanism the spectra of secondaries become significantly flatter at high energies $\varepsilon \gtrsim 100$ GeV/n. This effect can be directly studied from the secondary to primary (s/p) ratio: at high energies where reacceleration is important, the s/p ratio should be flatter than at lower energies.

Since positrons also represent the secondary CR component the formation of their energy spectrum should be very similar to the case of secondary nuclei. In particular if the standard model prediction is also valid for positrons one has to expect the flattering of positron energy spectrum at high energies.

It is therefore important to find the consistency of standard model prediction with the increase of positron to electron ratio at energies from 10 to 100 GeV detected in PAMELA [6] and Fermi-LAT [7, 8] satellite experiments. According to estimates of the spectrum of positrons created and accelerated in SNRs [9] such a consistency may exist. To find a strict conclusion one needs however to study the formation of electron and positron spectra based on the nonlinear time-dependent kinetic model including acceleration of positrons created in SNR and in the interstellar medium (ISM) as well.

Here we apply the same approach based on the kinetic nonlinear model of CR acceleration in SNRs, which was used for determination of the secondary nuclei spectra [5], in order to calculate the expected electron and positrons energy spectra and to compare them with the existing data.

2 Acceleration and reacceleration of CRs in SNRs

There are two different ISM suprathermal particle populations which are injected into the diffusive shock acceleration process in SNRs. The first and most general one is the injection of some fraction of the postshock thermal particle distribution. It occurs for all ions present in the background medium and usually supplies enough particles to convert a significant part of the SN shock energy into that of an energetic particle population.

The second possibility is the acceleration of pre-existing GCR particles which have a sufficiently high energy $\varepsilon \gtrsim 100$ MeV/n so that they participate naturally into the acceleration process. To distinguish these two different injection mechanism we use here the term "acceleration" for the first case and "reacceleration" for the second.

Proton injection is described in terms of dimensionless parameter η which is a fraction of the incoming thermal protons which are instantly involved into the acceleration at the gas subshock with a speed that exceeds the postshock gas sound speed c_{s2} by a factor $\lambda > 1$ [2]:

$$N_{\mathrm{inj}} = \eta N_{\mathrm{g1}}, \ p_{\mathrm{inj}} = \lambda m c_{s2}. \qquad (1)$$

Here $N_{\mathrm{g}} = \rho / m_{\mathrm{p}}$ is the gas number density, and the subscripts 1(2) refer to the point just ahead (behind) the shock. We assume that electrons are also injected into the diffusive shock acceleration process still at nonrelativistic energies below $m_{\mathrm{e}} c^2$. Since the electron injection mechanism is not very well known for simplicity we consider their acceleration starting from the same momentum as protons. At relativistic energies they have exactly the same dynamics as the protons. Therefore, neglecting synchrotron losses, their distribution function at any given time has the form

$$f_{\mathrm{e}}(p) = K_{\mathrm{ep}} f(p) \qquad (2)$$

for energies exceeding the electron injection energy, with some factor $K_{\mathrm{ep}} \ll 1$. The electron distribution function

$f_e(p)$ deviates only at sufficiently large momenta p from this relation due to synchrotron losses.

Since the spectra of GCRs have a peak at kinetic energy $\varepsilon = \varepsilon_{GCR} \approx 300$ MeV and in the case of reacceleration it is assumed that the existing GCR population is injected at the SN shock front into the diffusive acceleration with this energy

$$p_{inj} = p_{GCR}, \quad N_{inj} = N_{GCR}. \quad (3)$$

Here N_{GCR} is the total number of GCR species per unit volume and p_{GCR} is their mean momentum, that corresponds to ε_{GCR}.

In order to determine the number of reaccelerated CRs we starts from the case of protons. For this purpose we use the analytical approximation for their flux (differential intensity) in ISM (e.g. [11])

$$I(\varepsilon) = 1.93(v/c)[0.939 + (\varepsilon/1 \text{ GeV})] \quad (4)$$

in part/(cm^{2}s st). Here v and ε are the speed and kinetic energy of proton respectively, c is the speed of light. Integration of the expression $n = 4\pi I/v$ over the protons energies above 0.3 GeV gives the number density of CR protons $N_{GCR} = 3.3 \times 10^{-10}$ cm^{-3}.

Since at GeV energies the flux of CR electrons is by a factor of 100 lower then the protons and the flux of positrons is about 0.2 of electron flux the values of number density of CR electrons and positrons in ISM are $N_{GCR} = 3.3 \times 10^{-12}$ cm^{-3} and $N_{GCR} = 6.6 \times 10^{-13}$ cm^{-3} respectively.

There is an additional mechanism of secondary GCR production inside SNRs: primary nuclei like GCRs in the Galactic disk produce light secondary as a result of their nuclear collisions with the background gas. The total production rate of secondary electrons and positrons in SNRs due to the proton-proton collisions can be represented in the form [12]

$$Q_e(\varepsilon_e) = cN_g \int_{\varepsilon_e}^{\infty} \frac{d\varepsilon_p}{\varepsilon_p} \sigma_{in}(\varepsilon_p)N_p(\varepsilon_p)F_e(\varepsilon_e, \varepsilon_p), \quad (5)$$

where $N_p(\varepsilon_p)$ is differential proton number density. We use analytical expressions for the inelastic cross-section of proton-proton interaction $\sigma_{in}(\varepsilon_p)$ and for the function $F_e(\varepsilon_e, \varepsilon_p)$ derived in [12]. The source term $Q_e(\varepsilon_e)$ describes the creation of electrons and positrons throughout the remnant within wide energy range up to the energy $\varepsilon_e \sim 0.05\varepsilon_{max}$, where ε_{max} is the proton maximal energy. The particles created at distances less then the proton diffusive length $l(\varepsilon_p)$ from the shock front undergo subsequent acceleration. Since the diffusive length is increasing function of energy $l \propto \varepsilon_p$ acceleration makes the secondary particle spectra considerably harder compared with the spectra of primaries.

The spectrum of CRs in the ISM is $N_{GCR}(\varepsilon) = \tau(\varepsilon)N(\varepsilon)$, where $N(\varepsilon)$ is the spectrum of CRs released from SNRs, $\tau(\varepsilon)$ is the escape time from the Galaxy in the case of protons and $\tau(\varepsilon) \approx \tau_{loss}(\varepsilon)$ is the loss time $\tau_{loss}(\varepsilon) \propto 1/\varepsilon$ determined by inverse Compton scattering and synchrotron emission in the case of high energy electrons and positrons.

3 Results and discussion

In order to study the energy spectra of electrons and positrons produced in SNRs we have performed selfconsistent calculations of CR acceleration in SNRs, based on the
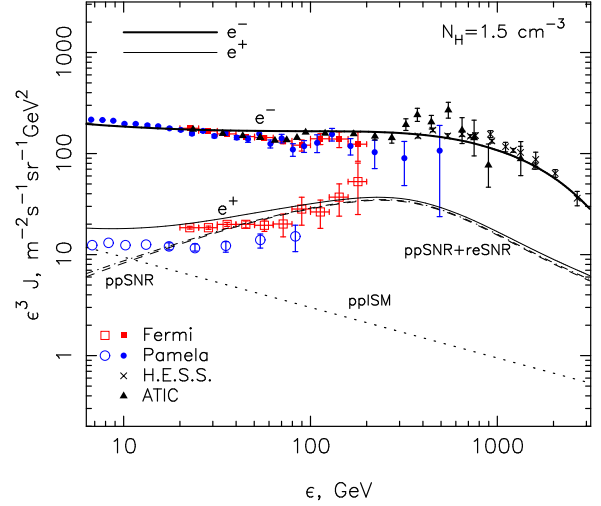
Figure 1: Calculated electron (thick line) and positron (thin lines) spectra produced inside SNRs in ISM of number density $N_H = 1.5$ cm^{-3} together with PAMELA [15, 16], Fermi LAT [17], HESS [18] and ATIC [19] data. Dotted (ppISM) and dashed (ppSNR) lines represent spectra of positrons created in p-p collisions in ISM [20] and inside SNR respectively, dash-dotted (reSNR) line represent the spectrum of positrons produced in SNRs.

kinetic nonlinear model, for the simple case of a uniform ISM with different densities.

We use the values $E_{SN} = 10^{51}$ erg for the explosion energy and $M_{ej} = 1.4M_\odot$ for the ejecta mass which are typical for SNe Ia in a uniform ISM. Note that the main fraction of the core collapse SNe has relatively small initial progenitor star masses between 8 and 15 $M_\odot$ which therefore do not significantly modify the surrounding ISM through the main sequence wind of the progenitor star. SNR evolution in this case is very similar to that of SNe Ia.

We adopt an injection rate of suprathermal protons, characterized by the injection parameters $\eta = 10^{-4}$ and $\lambda = 4$, which are expected for a typical SNR [13]. We consider three essentially different phases of the ISM: a diluted, hot ISM with hydrogen number density $N_H = 0.003$ cm^{-3} and temperature $T_0 = 10^6$ K, a warm ISM with $N_H = 0.3$ cm^{-3} and $T_0 = 10^4$ K, and an "average" ISM with $N_H = 1.5$ cm^{-3} and $T_0 = 10^4$ K. The ISM magnetic field values $B_0 = 3$ μG, 5 μG and 5 μG where taken for these three cases, respectively. Note, that at early SNR evolutionary phases magnetic field inside SNRs is expected to be considerably amplified. However since the secondaries are mainly produced at the late evolutionary phases [5] we ignore here this effect and use the time-independent upstream magnetic field value B_0.

GCRs at kinetic energy $\varepsilon \approx 1$ GeV are characterized by the electron to proton ratio $K_{ep} = 10^{-2}$. Since the main part of CRs produced in SNRs are released in the surrounding ISM at late Sedov SNR evolutionary phase the value $K_{ep} = 10^{-2}$ characterizes the injection of protons and electrons at this late stage. At the same time for all known young SNRs the value of this parameter extracted from the fit of the SNRs nonthermal emission properties is considerably lower: $K_{ep} \sim 10^{-4}$ (e.g. [14]). This situation suggests the increase of electron injection rate during SNR evolution so that electron to proton ratio $K_{ep}(t)$ is increasing function
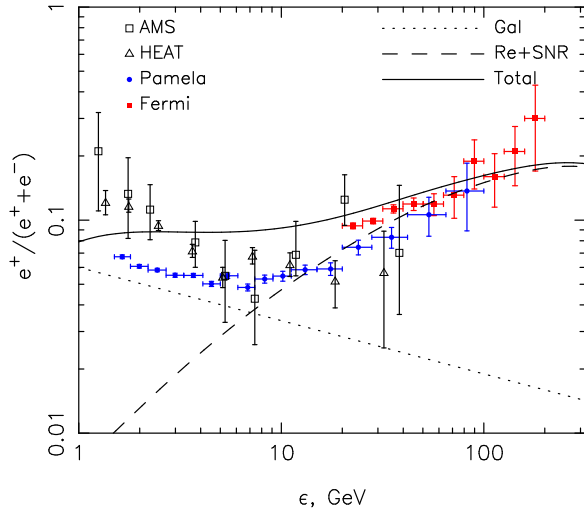
Figure 2: Calculated ratio of positron to electron produced inside SNRs in ISM of number density $N_H = 1.5$ cm^{-3} (dashed line) together with PAMELA [15, 16], Fermi LAT [17], HEAT, AMS-01 and new AMS-02 data. Dotted line represents the positron to electron ratio created in p-p collisions in ISM [20]. The solid line is the sum of this two components.

Figure 3: Antiproton to proton ratio as function of enrery. The dotted line is the ratio created in p-p collisions in ISM. The calculated ratio of reaccelerated (dash-dotted line) in SNR and reaccelerated plus created in p-p collisions in SNR (dashed line) $\bar{p}/p$ in ISM of number density $N_H = 1.5$ cm^{-3} are shown together with PAMELA data [21]. The solid line is the sum of above dotted and dashed lines.

of SNR evolutionary time t. We use in our calculations $K_{ep} \sim 10^{-4}$ at $t < 10^4$ yr and

$$\lg(K_{ep}) = -4 + 6.5 \lg(t/10^4 \text{ yr}) \qquad (6)$$

at $t > 10^4$ yr.

Calculated electron and positron spectra, produced inside SNRs situated in ISM of number density $N_H = 1.5$ cm^{-3} are presented in Fig.1 together with the existing data. It is seen that at energies from 10 to 200 GeV the calculated positron spectrum is considerably flatter then the electron spectrum. Electron and positron spectra are in a satisfactory agreement with the results of recent experiments.

Since the production rate of secondary electrons and positrons in p-p collisions is proportional to the gas density the number of positrons with energies $\varepsilon > 10$ GeV produced in SNRs is lower at lower ISM density $N_H < 1.5$ cm^{-3} compared with the case of $N_H = 1.5$ cm^{-3}.

Similar calculations made for production of secondary anpiprotons. The result for $N_H = 1.5$ cm^{-3} are presented in Fig.3

4   Summary

Since $N_H = 1.5$ cm^{-3} well corresponds to the mean gas number density within the Galactic disk we conclude that the observed electron and positron spectra can indeed be produced in Galactic SNRs.

References

[1] Berezhko E. G. and Völk H. J. 2007, Astrophys. J., 661, L175
[2] Berezhko E. G., Elshin V. K., and Ksenofontov L. T. 1996, J. Exp. Theor. Phys., 82, 1
[3] Berezhko E. G. and Völk H. J. 1997, Astropat. Phys., 7, 183
[4] Zirakashvili V. N. and Aharonian F. A. 2010, Astrophys. J., 708, 965
[5] Berezhko E. G. et al. 2003, Astron. Astrophys., 410, 189
[6] Adriani O. et al. [PAMELA Collaboration] 2009, Nature, 458, 607
[7] Abdo et al. [The Fermi LAT Collaboration] 2009, Phys. Rev. Lett., 102, 181101
[8] Ackermann et al. [The Fermi LAT Collaboration] 2010, Phys. Rev. D, 82, 092004
[9] Blasi P. 2009, Phys. Rev. Lett., 103, 051104
[10] Blasi P. 2009, Phys. Rev. Lett., 103, 081103
[11] Berezinsky V. S. et al. 1990 *Astrophysics of cosmic rays* (Amsterdam: North-Holland)
[12] Kelner S. R., Aharonian F. A. and Bugayov V. V. 2006, Phys. Rev.D, 74, 034018
[13] Völk H. J., Berezhko E. G. and Ksenofontov L. T. 2003, Astron. Astrophys., 409, 563
[14] Berezhko E. G. 2008, Adv. Space Sci., 41, 429
[15] Adriani O. et al. [PAMELA Collaboration] 2011, Phys. Rev. Lett., 106, 201101
[16] Mocchiutti E. et al. [PAMELA Collaboration] 2011, Proc. 32nd ICRC, Beijing, 6, 64
[17] Ackermann et al. [The Fermi LAT Collaboration] 2012, Phys. Rev. Lett, 108, 011103
[18] Aharonian F. et al. [The HESS Collaboration] 2008, Phys. Rev. Lett., 101, 261104
[19] Chang J. et al. [The ATIC Collaboration] 2008, Nature, 456, 362
[20] Moskalenko I. V. and Strong A. W. 1998, Astrophys. J., 493, 694
[21] Donato F. et al., 2009 Phys. Rev. Lett. 102, 071301